



Supplement of

The density of ambient black carbon retrieved by a new method: implications for cloud condensation nuclei prediction

Jingye Ren et al.

Correspondence to: Fang Zhang (zhangfang2021@hit.edu.cn)

The copyright of individual parts of the supplement might differ from the article licence.

23 **Methods and theory for CCN number concentration prediction**

24 **Assumption 1: BC internally mixed**

25 BC particles are assumed to be internally mixed with bulk chemical composition,
26 when using a density of BC with the value of 2.1 g cm^{-3} in the sensitivity test. For this
27 scheme, six species are considered, ie., NH_4HSO_4 , $(\text{NH}_4)_2\text{SO}_4$, NH_4NO_3 , POA, SOA
28 and BC. By applying the hygroscopicity parameter κ_{chem} into κ -Köhler relationship
29 (Petters & Kreidenweis, 2007), the critical diameter or activation diameter (D_{cut}) can be
30 obtained at a given supersaturation (S). Thus, the CCN concentration can be predicted
31 by using the critical diameter and particle number size distribution.

32 The equations used in the estimating N_{CCN} are as follows,

$$33 \quad \text{CCN}_{pre} = \int_{D_{cut}}^{D_{end}} n(\log D_p) d \log D_p \quad (1)$$

34 where D_{cut} is the critical diameter, D_{end} is the upper size limit of the particle number size
35 distribution (PNSD), $n(\log D_p)$ is the function of the aerosol number size distribution.

$$36 \quad D_{cut} = \sqrt[3]{\frac{4A^3}{27\kappa \ln^2 S}}, \quad A = \frac{4\sigma_{s/a}M_w}{RT\rho_w} \quad (2)$$

37 where κ is the hygroscopicity parameter, S is a given supersaturation, M_w is the
38 molecular weight of water, $\sigma_{s/a}$ is the surface tension of pure water, ρ_w is the density of
39 water, R is the gas constant, and T is the absolute temperature. Here the parameters T
40 and ρ_w were adjusted to standard conditions ($T=298.15\text{K}$).

41 **Assumption 2: BC externally mixed**

42 When using a density of 0.14 g cm^{-3} in the sensitivity test, BC particles are
43 assumed to be externally mixed but other five species are treated as internally mixed,

44 ie., NH_4HSO_4 , $(\text{NH}_4)_2\text{SO}_4$, NH_4NO_3 , POA and SOA. The CCN number concentration
45 of the internal mixture is denoted as $N_{\text{CCN_In}}$. The way to retrieve the critical diameter
46 (D_{cut}) is same as the assumption 1. The difference is that the $N_{\text{CCN_In}}$ should be
47 multiplied by the volume fraction of the internal mixed particles to get the finally N_{CCN}
48 (Ren et al., 2018). The CCN concentration can be calculated as follows:

$$49 \quad CCN_{pre_IN} = \left(\int_{D_{cut}}^{D_{end}} n(\log D_p) d \log D_p \right) \cdot VF \quad (3)$$

50 where VF is the volume fraction of the internally mixed components. The other
51 parameters are same as those presented in Eqs. 1-2.

52 **Assumption 3: aged BC internally mixed but fresh BC externally mixed**

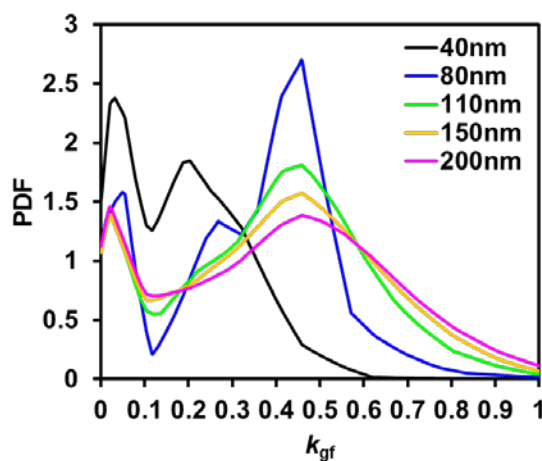
53 In this assumption, the fresh BC and POA are externally mixed but sulfate, nitrate
54 and SOA with the aged BC particles are internally mixed. The mass fraction of
55 internal/aged BC and external/fresh BC are retrieved from 2.2. Similar to the
56 assumption 2, the CCN concentration is calculated by using the critical diameter and
57 the PNSD. And the CCN number concentration also should be multiplied by the volume
58 fraction of five internal species. The equation is the same as Eqs. 3. The other
59 parameters are same as those presented in Eqs. 1-3. By varying the densities of internal
60 and external BC particles, a CCN closure test has been done based on this assumption.
61 Then the optimal density of internal and external BC is obtained when the best estimates
62 of N_{CCN} are achieved.

63 **References**

64 Petters, M. D., & Kreidenweis, S. M.: A single parameter representation of hygroscopic
65 growth and cloud condensation nucleus activity, *Atmospheric Chemistry and Physics*,
66 7(8), 1961-1971, <https://doi.org/10.5194/acp-7-1961-2007>, 2007.

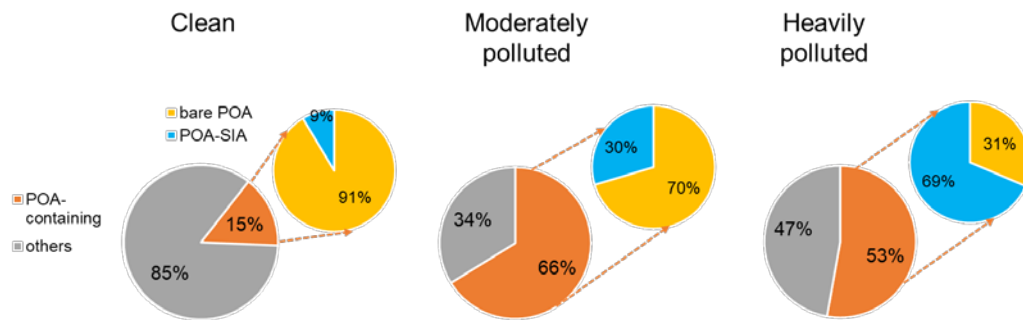
67 Pang, Y., Chen, M., Wang, Y., Chen, X., Teng, X., Kong, S., et al.: Morphology and
68 fractal dimension of size-resolved soot particles emitted from combustion sources.
69 Journal of Geophysical Research: Atmospheres, 128, e2022JD037711. <https://doi.org/10.1029/2022JD037711>, 2023.
70
71 Ren, J., Zhang, F., Wang, Y., Collins, D., Fan, X., Jin, X., et al.: Using different
72 assumptions of aerosol mixing state and chemical composition to predict CCN
73 concentrations based on field measurements in urban Beijing, Atmospheric
74 Chemistry and Physics, 18, 6907–6921, <https://doi.org/10.5194/acp-18-6907-2018>,
75 2018.
76 Liu, L, Zhang, J, Zhang, Y, Wang, Y, Xu, L, Yuan, Q, et al.: Persistent residential
77 burning-related primary organic particles during wintertime hazes in North China:
78 insights into their aging and optical changes, Atmos. Chem. Phys. 21, 2251–2265,
79 <https://doi.org/10.5194/acp-21-2251-2021>, 2021.
80 Xie, Y.Y., Ye, X.N., Ma, Z., Tao, Y., Wang, R.Y., Zhang, C., et al.: Insight into winter
81 haze formation mechanisms based on aerosol hygroscopicity and effective density
82 measurements, Atmospheric Chemistry and Physics, 17(11), 7277-7290,
83 <https://doi.org/10.5194/acp-17-7277-2017>, 2017.
84 Zhang, Y., Su, H., Ma, N., Li, G., Kecorius, S., Wang, Z., et al.: Sizing of ambient
85 particles from a single-particle soot photometer measurement to retrieve mixing state
86 of black carbon at a regional site of the North China Plain. Journal of Geophysical
87 Research: Atmospheres, 123, 12,778–12,795, <https://doi.org/10.1029/2018JD028810>, 2018.
88

89 Figures



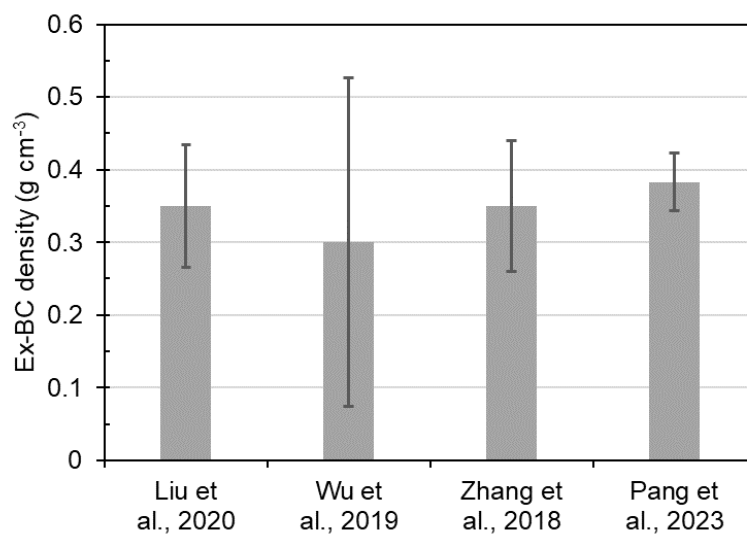
90

91 **Figure S1.** Average κ -PDF patterns of particles in different sizes.



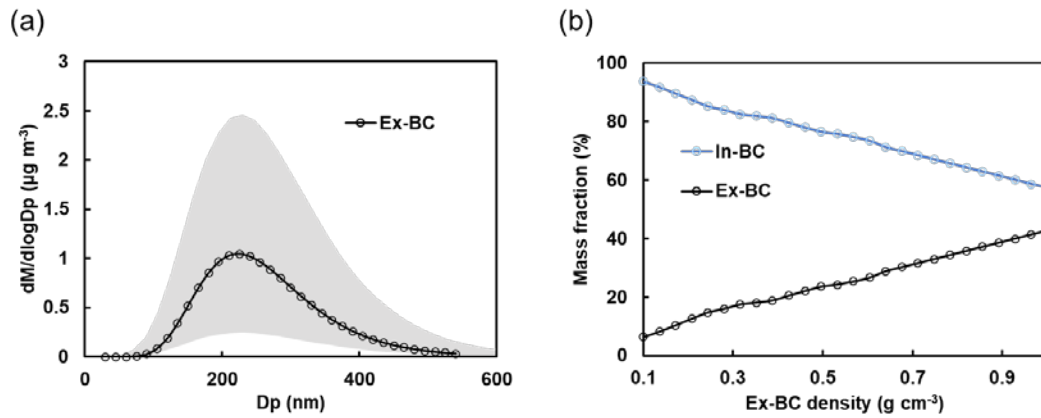
92

93 **Figure S2.** Average number fractions of POA-containing and bare POA under clean
 94 ($PM_{2.5} \leq 75 \mu g m^{-3}$), moderately ($75 < PM_{2.5} \leq 200 \mu g m^{-3}$), and heavily polluted
 95 ($PM_{2.5} > 200 \mu g m^{-3}$) conditions in the winter of 2016 at BJ site (referred from Liu et al.,
 96 2021).



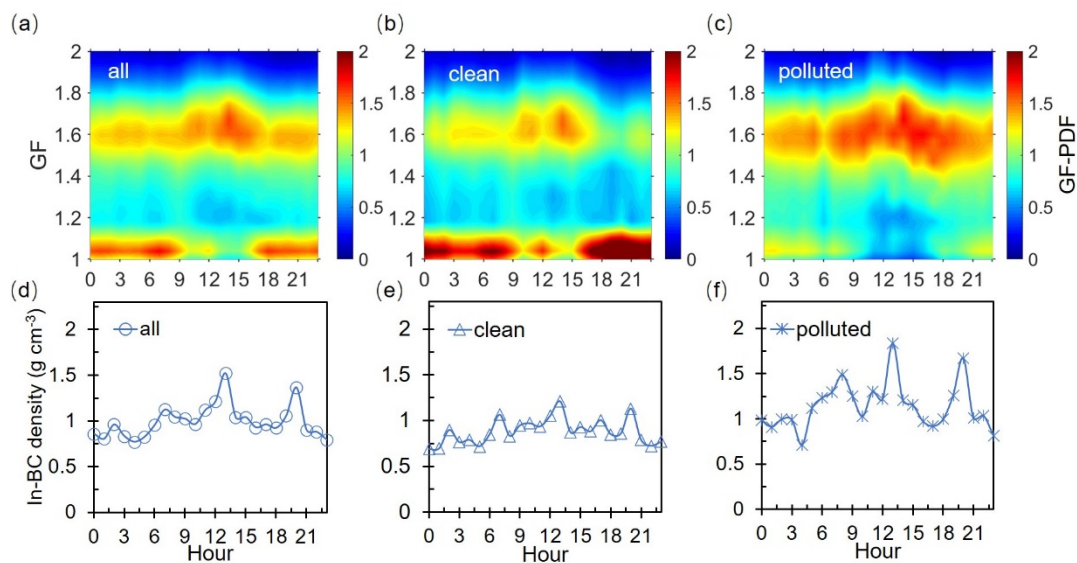
97

98 **Figure S3.** Summary of the ambient externally mixed BC density particles in North
 99 China Plain from literatures.



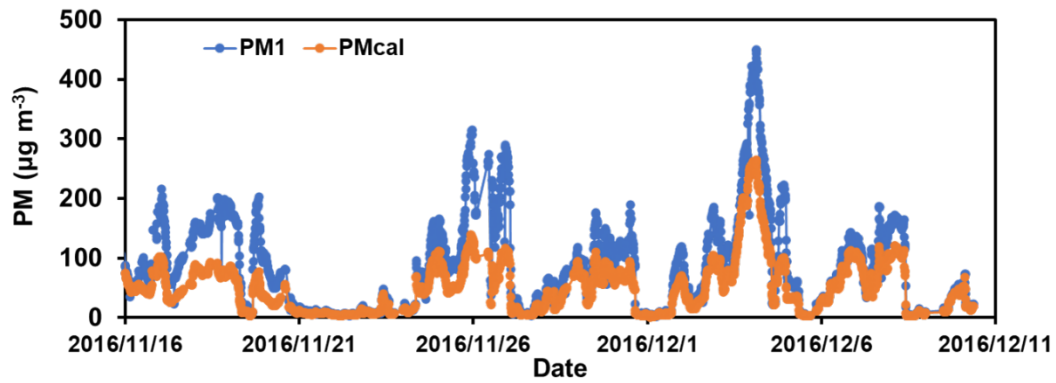
100

101 **Figure S4.** (a) Average mass size distribution of Ex-BC by modeling as a single log-
 102 normal distribution. The shaded part represents the boundary by setting the Ex-BC
 103 density as 0.1 g cm^{-3} (lower limit) and 1.0 g cm^{-3} (upper limit). (b) Mean mass fraction
 104 of In-BC and Ex-BC by increasing the $\rho_{\text{Ex-BC}}$ from 0.1 to 1.0 g cm^{-3} .



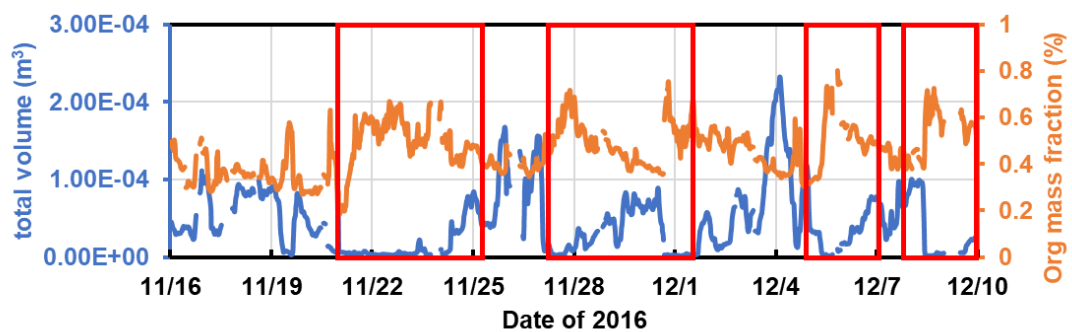
105

106 **Figure S5.** Diurnal variations in GF-PDFs for 200 nm particles and In-BC density for
 107 the campaign-averaged (a and d), clean ($\text{PM}_{2.5} \leq 75 \text{ µg m}^{-3}$) (b and e) and polluted
 108 periods ($\text{PM}_{2.5} > 75 \text{ µg m}^{-3}$) (c and f).



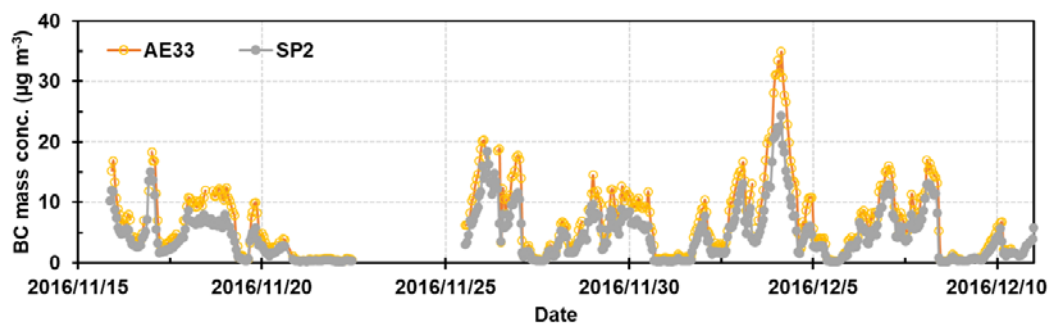
109

110 **Figure S6.** Temporal evolutions of PM₁ concentration (measured with an Aerosol
 111 Chemical Speciation Monitor, ACSM and calculated PM_{cal} (measured with a scanning
 112 mobility particle sizer, SMPS). The effective density of PM₁ was assumed to be 1.5 g
 113 cm⁻³ in the range of 10–550 nm measured (Xie et al., 2017).



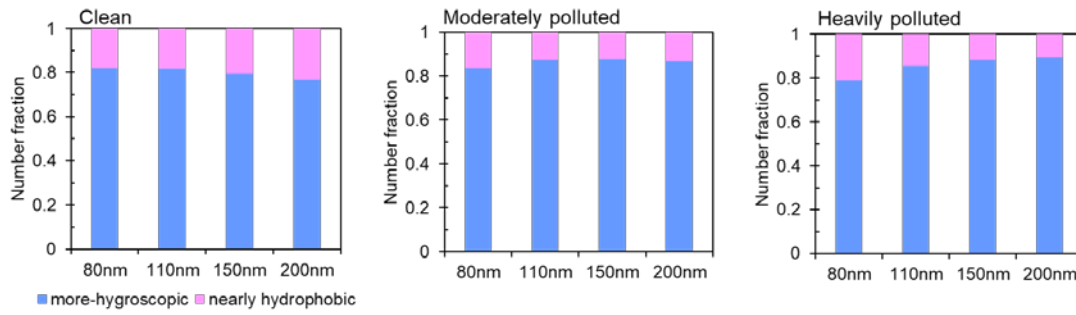
114

115 **Figure S7.** Time series of the calculated total volume of PM₁ and mass fraction of
 116 organics.



117

118 **Figure S8.** Time series of mass concentration of BC measured by AE33 and SP2.



119

120 **Figure S9.** Campaign-averaged number fraction of nearly hydrophobic and more

121 hygroscopic groups for 80-200 nm particles under clean, moderately, and heavily

122 polluted conditions.